Fluid-structure interaction modelling of propellant combustion

C. Tsangalis* N. McLachlan* P. Trivailo*

(Received 21 October 2005; revised 4 September 2006)

Abstract

The controlled combustion of solid propellants is vital to rocket motor design, weapon system design and gas generators used for airbag inflation and fire suppression. Given the characteristics of any propellant and structural system, a model of combustion should be able to establish the energy release and corresponding pressure generated by the propellant on the system. Due to inherent complexities associated with propellant ignition and combustion, the description of propellant burn and consequent impact on structural design is not well understood. This article investigates the nature of propellant burn through the development of a computer simulated model. More specifically, governing equations of solid propellant combustion based on the Nobel–Abel equation of state are introduced into a finite element environment to perform fluid-structure interaction modelling on

*School of Aerospace, Mechanical and Manufacturing Engineering, RMIT University, Melbourne, Australia. mailto:S9908736@student.rmit.edu.au

See http://anziamj.austms.org.au/V47EMAC2005/Tsangalis for this article, Published October 16, 2006. ISSN 1446-8735

the system. The Nobel–Abel Equation of State in conjunction with a steady state burning law, which describes the recession rate of the burning propellant, is incorporated into a finite element environment through a user subroutine. The fluid-structure interaction capabilities allowed for the impact of the evolving gasses on the structure of the system to be analysed. The derived model empowered the analysis of a wide range of system parameters their effect on system performance. Results of material stress/strain and fluid dynamics are presented.

Contents

1 Introduction

Understanding the process of combustion is vital to the design and analysis of various engineering applications. For example, propellant combustion is vital to rocket motor design, weapon system design and gas generators used

Table 1: Nomenclature

$A_s =$	bore cross sectional area	mm^2
$B =$	burn rate coefficient	$\mathrm{mm\,s}^{-1}$
$C =$	charge weight	tonne
$D =$	diameter of grain	mm
$g_c =$	unit conversion factor	
$L =$	length of grain	mm
$M_E =$	effective mass	tonne
$N =$	number of perforations	
$n =$	burn rate exponent	For MPa
$n' =$	mass of gas	tonne
$P_A =$	average pressure	MPa
$P_B =$	piston base pressure	MPa
$R =$	gas constant	$\mathrm{mJ\,tonne}^{-1}{}^{\circ}\mathrm{K}^{-1}$
$r =$	perforation radius	mm
$R' =$	piston radius	mm
$S =$	piston travel	mm
$T_0 =$	Flame temperature	$^{\circ}$K
$V_T =$	total volume	mm^3
$V_{c0} =$	initial chamber volume	mm^3
$V_p =$	velocity	$\mathrm{mm.s}^{-1}$
$W_s =$	piston weight	tonne
$x =$	linear recession of grain	mm
$Z =$	fraction of charge burnt	
$\beta =$	heat-loss adjustment factor	
$\gamma =$	specific heat ratio	
$\eta =$	gas covolume	$\mathrm{mm}^3\mathrm{tonne}^{-1}$
$\lambda =$	force constant	$\mathrm{mJ\,tonne}^{-1}$
$\rho_s =$	solid propellant density	$\mathrm{tonne\,mm}^{-3}$

for airbag inflation and fire suppression. Much literature exists [1, 4, 8] in which the combustion behavior of various propellants are simulated.

In any combustion system, there exists a set of fixed and variable factors which ultimately affect performance. Fixed factors are generally related to the structural properties of the system and often these are difficult to manipulate without requiring a total redesign and manufacture of structural components. More conveniently, variable factors associated with the propellant can be modified to improve performance.

The variation of propellant charge offers significant and convenient means of manipulating system performance. Propellant type, configuration and quantity can be varied in order to achieve a particular burn cycle and hence a desired performance. Various models exist in which structural and propellant properties are used to predict the performance of combusting systems. One such model is proposed by Krier et al. [3] in which the Nobel–Abel Equation of State is used to establish the energy release and corresponding pressure generated by the combusting propellant.

The Nobel–Abel Equation of State is of the covolume type and is generally used as a good first approximation in the formulation of interior ballistic problems. In simplest form, the Nobel–Abel Equation of State is

$$(P/n')\,(V - n'\eta) = RT_0\,, \tag{1}$$

where

$$\begin{aligned} n' &= \text{mass of gas (tonnes)}, \\ \eta &= \text{gas covloume } (\text{mm}^3\,\text{tonne}^{-1}), \\ R &= \text{gas constant } (\text{mJ}\,\text{tonne}^{-1\circ}\text{K}^{-1}). \end{aligned}$$

Other authors also utilised the Nobel–Abel Equation of State in ballistics applications. Papliski et al. [5] discuss thermodynamical extensions to the Nobel–Abel Equation of State to describe properties of combustion products for given propellants. Johnston [2] uses the Nobel–Abel Equation of State

and derives additional thermodynamic functions for ballistics modelling using computational fluid dynamics solvers. Here, Krier's ballistic model is incorporated into the finite element environment through a user subroutine. The resulting fluid-structure interaction model simulates the fluid dynamics of the propellant and its impact on the structural system.

2 The combustion model

The model proposed by Krier was first solved in MATLAB in order to asses the influence of various parameters on the performance of the system. The MATLAB model was also used to ensure that the user defined subroutine was functioning correctly in the finite element software. The simulation involved the combustion of granular multi-perforated propellant in a closed volume in order to investigate the resultant pressure rise. Others, such as Pocock et al. [6] and Ritchie et al. [7], also considered the performance of perforated propellant grains using numerical methods.

As the ignition process is quite complex, it was not treated with any detail in this investigation. Instead, the simulation assumed that simultaneous and uniform ignition of all propellant grains always occurred.

Krier's model is intended for the analysis of weapon systems and therefore considers the pressure rise in an expanding volume where it is expected that a projectile (or piston) would be expelled from a cylinder. Whereas Krier [3] gives a full discussion of his model, the following equations and initial conditions were utilised in this investigation to construct the combustion model.

Propellant Burning Rate Law:

$$\frac{dx}{dt} = BP_A^n \,. \tag{2}$$

Piston Acceleration:

$$\frac{dV_p}{dt} = \frac{P_B A_s}{W_s} \,. \tag{3}$$

Piston Travel:

$$\frac{ds}{dt} = V_p = \int_0^t \left(\frac{dV_p}{d\tau}\right) dt \,. \tag{4}$$

Total Chamber Volume (including propellant and gas volumes):

$$V_T(t) = V_{c0} + A_s S(t) - C\left\{(1/\rho_s) + Z\left[\eta - (1/\rho_s)\right]\right\} \,, \tag{5}$$

where

$$Z = \frac{2\left[cL + d\right]x - \left[L(1-n) + 4c\right]x^2 + 2(1-n)x^3}{Ld} \,,$$

and

$$c = R + nr \,, \quad d = R^2 - nr^2 \,.$$

Average Gas Pressure (with heat loss):

$$P_A = \frac{\lambda C Z - (\gamma - 1)(1+\beta)\left(M_E V_p^2/2\right)}{V_T(t)} \,, \tag{6}$$

where

$$M_E = W_s + (CZ/3) \,.$$

Pressure Conversion (base to average):

$$P_B : P_A = \left[1 + \frac{\gamma - 1}{2}\frac{V_p^2}{g_c \lambda}\right]^{-\gamma/(\gamma-1)} \,. \tag{7}$$

Initial Values:

$$X(0) = X_0 \,, \quad \text{[a small number of order } 10^{-3} \text{ in.,]} \tag{8}$$

$$V_p(0) = 0 \,, \tag{9}$$

$$S_p(0) = 0 \,, \tag{10}$$

$$V_T(0) = V_{c0} - (C/\rho_s) \,, \quad \text{[approximate due to condition (8).]} \tag{11}$$

TABLE 2: system parameters for closed volume simulation.

Parameter	Symbol	Value	Units
Propellant properties			
length of grain	L	6.13	mm
diameter of grain	D	3.12	mm
number of perforations	N	1	
perforation radius	r	0.255	mm
solid propellant density	ρ_s	1.45e-9	$\text{tonne}\,\text{mm}^{-3}$
charge weight	C	0.00005	tonne
specific heat ratio	γ	1.2582	
force constant	λ	9.41e11	$\text{mJ}\,\text{tonne}^{-1}$
gas constant	R	364.5e6	$\text{mJ}\,\text{tonne}^{-1}{}^{\circ}\text{K}^{-1}$
gas covolume	η	1.06e9	$\text{mm}^3\text{tonne}^{-1}$
burn rate coefficient	B	0.732	$\text{mm}\,\text{s}^{-1}$
burn rate exponent	n	0.952	For MPa
Structural properties			
closed volume	V_T	2.759e5	mm^3

The ballistic model is solved by simultaneously integrating Equations (2–4), utilising Equations (5–7) and specified initial conditions. Note that Equation (3) was simplified for a smooth bore cylinder as compared to the reference which considers a rifled barrel.

As we only considered a closed volume to begin the investigation, terms relating to piston acceleration and travel were ignored. Table 2 contains a set of system parameters utilised in the simulation.

3 Results

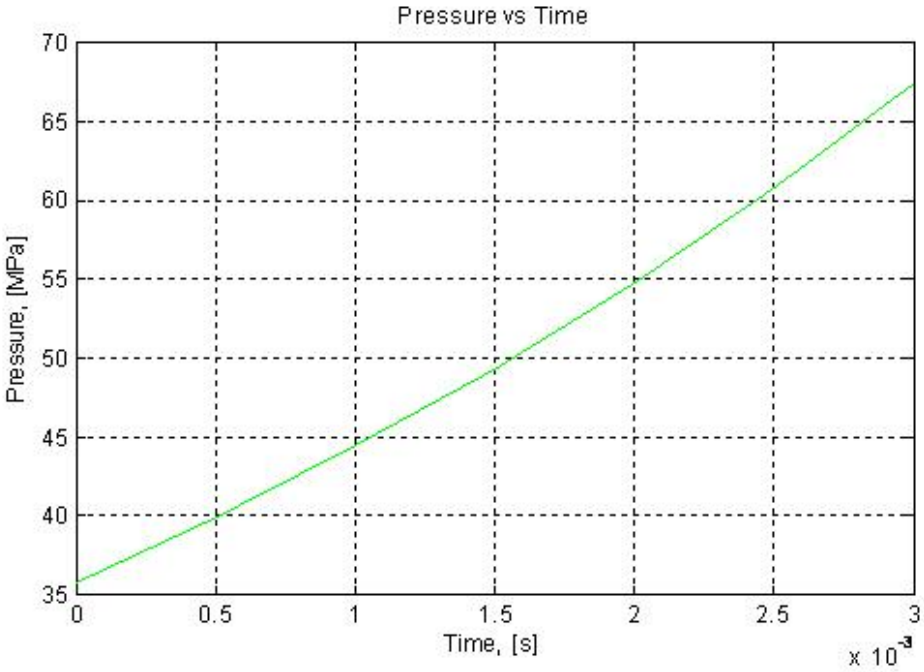

FIGURE 1: pressure versus time relationship for propellant combustion in closed volume

3.1 MATLAB analysis

Figure 1 demonstrates the predicted pressure rise in a closed volume for perforated granular propellant, the properties of which are given in Table 2.

3.2 Finite element analysis

In order to define the combustion model in the finite element environment it was necessary to create a user subroutine. As DYTRAN was to be used to perform the analysis, it was necessary to adapt the MATLAB code to FOR-

```
*   Calculate Burn Fraction
*************************************************
*
      ZF(NZ)=((2*((c*L)+d)*X(NZ))-(((L*(1-nperf))+(4*c))*
     +        ((X(NZ))**2))+(2*(1-nperf)*((X(NZ))**3)))/(L*d)
*
*
*   Calculate New Pressure
*************************************************
*
      PNEW(NZ)=(lamda*XMASS(NZ)*Z(NZ))/(RELV(NZ)-
     +          ((XMASS(NZ)/rho_s)*(1-Z(NZ)))-(cvol*Z(NZ)*XMASS(NZ)))
*
*
*   Calculate New X
*************************************************
*
      X(NZ)=X(NZ)+DLTH*B*(PNEW(NZ))**EXP
```

FIGURE 2: main loop of user subroutine

TRAN 90 language for use with DYTRAN. When adapting the code, it was only necessary to include statements relating directly to the propellant as any structural properties were entered directly into DYTRAN. Therefore Equations (3–5) and (7) were omitted from the user subroutine.

Figure 2 illustrates the equations utilised in the main loop of the user subroutine. In the finite element analysis, the combustion model was applied to each individual element, as opposed to the MATLAB simulation where it was computed over the entire volume. Information relating to element volume and mass (which represents the charge weight) were retrieved directly from DYTRAN throughout the simulation run and can be seen as RELV and XMASS in Figure 2 respectively. The NZ term represents the element numbers assigned by DYTRAN and the loop is constructed such that each equation is computed for all the elements defined by the user subroutine.

The FE analysis was used to replicate the results produced in MATLAB. A simple cube mesh composed of solid Eulerian elements was constructed in the PATRAN pre-processor with the same volume as that used in the MATLAB analysis. No boundary conditions were required as DYTRAN automatically

assumes that any external Eulerian mesh surfaces act as a boundary to the flow.

The results produced by DYTRAN for pressure in the closed volume were identical to those displayed in Figure 1. It would be expected that DYTRAN could enable further accuracy of results as the time steps utilised in FE solvers are generally orders of magnitudes smaller than those utilised when running MATLAB simulations resulting in more precise integration schemes. It was also proven that in this case mesh density did not affect the simulation as identical results were produced using 1 element and 125 elements. In more advanced simulations, possibly incorporating expanding volumes or more eccentric geometries, mesh density would be a vital variable in accurately representing the flow of material. In such models, both the unburnt propellant and combustion gases would disperse unevenly throughout the chamber volume resulting in an irregular distribution of pressure.

3.3 Fluid structure interaction modelling

By introducing the combustion model into the finite element environment it was possible to investigate the impact of fluid dynamics, involved in propellant combustion, on structural systems. This was achieved by performing fluid-structure interaction modelling where the DYTRAN Solver would compute the pressures generated in the combusting medium and then apply these to the surrounding structural system via coupling surfaces.

In order to demonstrate this capability a simple model was created in which propellant would be combusted inside a closed aluminium box. A half model was utilised in the simulation to allow visual inspection of the pressures generated inside the box. The appropriate boundary conditions were applied to the symmetry plane.

The gas was modelled using solid Eulerian elements, whereas the box was modelled using Lagrangian elements. In the simulation, the Eulerian

elements remain fixed and material is able to flow through them while the Lagrangian mesh moves according to material flow. To allow fluid-structure interaction it was necessary to overlap the two different meshes and define a coupling surface on the internal surface of the Lagrangian elements. At the beginning of the simulation, the overlapped Eulerian mesh contains no material and is considered to be a void space as the coupling surface acts as a boundary to the flow. The overlapping mesh allows deformation in the Lagrangian mesh and the attached coupling surfaces without loss of the coupling to the eulerian elements.

In DYTRAN, it is required that the coupling surface forms a closed volume in order for the coupling algorithms to work. As we were dealing with a half model, this became an issue as there were no Lagrangian elements on the symmetry plane with which to build a coupling surface. It was therefore necessary to construct a series of dummy elements of negligible stiffness on the symmetry plane. The nodes of these elements were locked in the direction normal to the symmetry plane to maintain the symmetry conditions of the model. However, the negligible stiffness ensured that the behaviour of the structure would not be affected by these elements. Figure 3 contains the finite element model of the closed box simulation. Image A shows the Lagrangian box only, Image B includes the Eulerian mesh and demonstrates the overlapped region and Image C shows the addition of the dummy elements.

The system parameters from Table 2 were again utilised for the simulation. The box was modelled using aluminium with an elastic modulus of 70 GPa, a density of 2.8 g/cc and a yield stress of 250 MPa. The results of the simulation can be seen in Figure 4. Column A shows the pressures generated by the propellant, Column B illustrates the stresses in the aluminium box and Column C shows the deformation of the aluminium box.

Figure 4 clearly demonstrate the pressure rise in the combusting propellant, the resultant stressing of the aluminium box beyond yield, and the consequent deformation of the structure. Early in the simulation we notice pressure waves developing in the gas with four distinct regions of high pres-

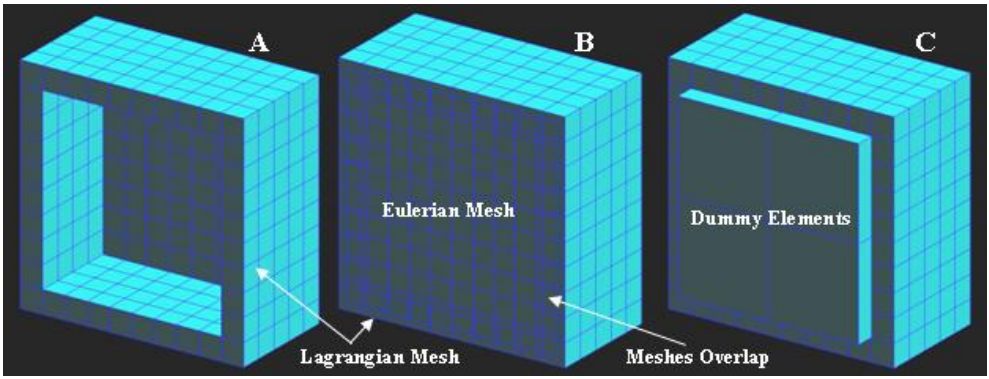

FIGURE 3: finite element model of closed box simulation: A, Lagrangian box only; B, Lagrangian and Eulerian mesh with overlapped region; C, entire model with dummy elements.

sure on the symmetry plane. This is followed by more erratic and turbulent conditions beyond 1 msec except for the rear corners of the box where we see distinct pressure drops. Column B demonstrates that the yield stress of the material is reached within 0.5 msecs as the box begins to plastically deform and continues to do so as more of the structure reaches its yield under the increasing pressure. These results offer significantly more insight as opposed to those produced by MATLAB, where an average pressure would be computed for the entire gas.

4 Discussion

Fluid-structure interaction modelling enabled the combustion of propellant to expand a closed box through the use of coupling surfaces and overlapping meshes. However, the deformation in this model did not exceed one element thickness. Modelling the combustion of propellant in large expanding volumes, where overlapping meshes will be many rows of elements thick, will

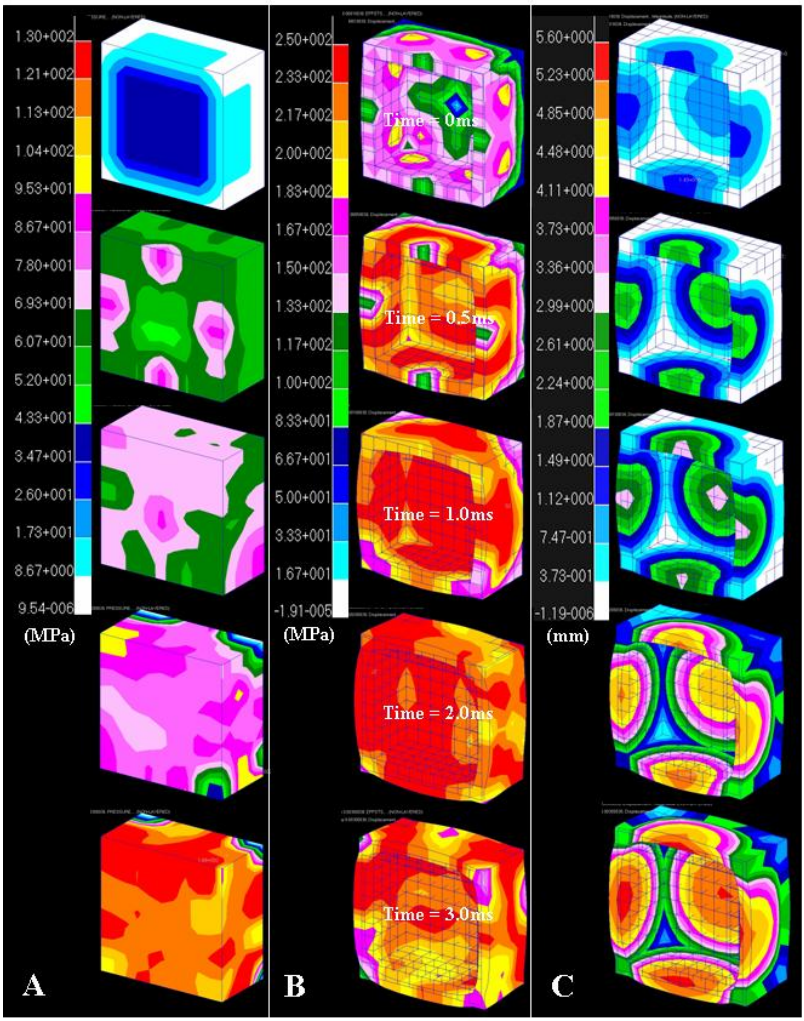

FIGURE 4: fluid-structure interaction results: A, gas pressure (Eulerian mesh shown only); B, material stress (Lagrangian mesh shown only); and C, material deformation (Lagrangian mesh shown only).

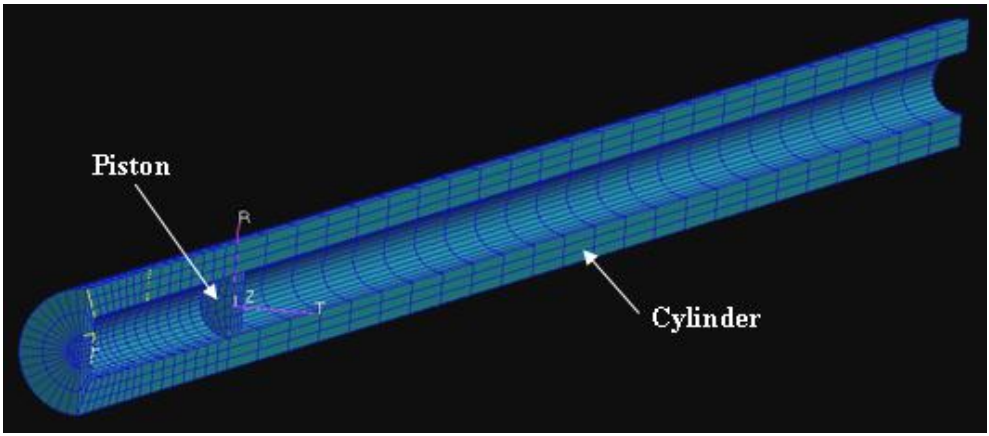

FIGURE 5: piston model.

require new and originally void Eulerian elements to be introduced into the analysis. These are filled by the gas/propellant mixture as coupling surfaces are displaced.

For example, Figure 5 shows a piston located inside a cylinder where the combustion of propellant would be used to push the piston. While the Eulerian elements are not shown in the figure, as the piston travels down the cylinder and through the Eulerian mesh, more Eulerian elements are filled by the gas/propellant mixture. To perform such an analysis will require the dynamic specification of conditions on newly introduced Eulerian elements equivalent to those possessed by immediately adjacent elements.

5 Conclusion

This investigation successfully introduced a ballistic model into a finite element environment. A user subroutine defining the Nobel–Abel Equation of State was incorporated into the DYTRAN explicit solver. It enabled the

analysis of structural behaviour subject to the fluid dynamics of propellant combustion through the use of fluid-structure interaction modelling.

Results generated in MATLAB for the combustion model were first replicated in DYTRAN using a basic cube mesh of Eulerian elements defined by the user subroutine. The investigation was then expanded to include the interaction of Lagrangian and Eulerian elements such that the pressures generated by the propellant would be used to stress the Lagrangian elements. This was demonstrated by simulating the combustion of propellant in a closed aluminium box, causing the box to expand under the pressure generated by the propellant.

Future work requires the combustion of propellant in large expanding volumes where new and originally void Eulerian elements are introduced into the analysis. This capability would provide significant scope to the design and analysis of various engineering applications including weapon systems and combustion engines.

References

[1] Buckmaster, J., Jackson, T. L., Massa, L. and Ulrich, M. , Response of a burning heterogeneous propellant to small pressure disturbances. *Proceedings of the Combustion Institute*, Vol. 30, Issue 2, pp.2079–2086, 2005. C391

[2] Johnston, I. A., The Nobel–Abel equation of state: thermodynamic derivations for ballistics modelling. South Australia, Defence Science and Technology Organisation, DSTO-TN-0670, 2005. C391

[3] Krier, H. and Adams, M. J., An introduction to gun interior ballistics and a simplified ballistic code. *Interior Ballistics of Guns*, American Institute of Aeronautics and Astronautics, New York, pp.1–36, 1979. C391, C392

[4] Massa, L., Jackson, T. L., Buckmaster, J., Ulrich, M. and Zhou, X., Exploring propellant science using a fully coupled combustion code. AIAA Paper No. 2003-1165, January 6–10, in *41th Aerospace Sciences Meeting & Exhibit*, Reno, Nevada, 2003. C391

[5] Papliski, A., Leciejewski, Z. and Surma, Z., About Thermodynamical Adjustment of the Nobel–Abel Equation of State *21st International Symposium on Ballistics*, Adelaide, South Australia, Defence Science and Technology Organisation, 2004. C391

[6] Pocock, M. D., Locking, P. M. and Guyott, C. C., Effect of statistical variation in grain geometry on internal ballistics modelling. *21st International Symposium on Ballistics*, Adelaide, South Australia, Defence Science and Technology Organisation, 2004. C392

[7] Ritchie, S.J., Lusk, P. D. and Domen, J. K., Performance prediction of 120mm gun propellants with a ballistic simulator. *18th International Symposium on Ballistics*, San Antonio, Texas, Technomic Publishing Company, Inc., 1999. C392

[8] Zhou, X., Jackson, T. L. and Buckmaster J. Oscillations in propellant flames with edges. *Combustion and Flame*, Vol. 133, pp.157–168, 2003. C391